June 10, 2010

Effect of Nanoparticle Surface Charge at the Plasma Membrane and Beyond

RR Arvizo
OR Miranda
MA Thompson
CM Pabelick
R Bhattacharya, et al.

NANO LETTERS

pubs.acs.org/NanoLett

Effect of Nanoparticle Surface Charge at the Plasma Membrane and Beyond

Rochelle R. Arvizo,[†] Oscar R. Miranda,[⊥] Michael A. Thompson,[‡] Christina M. Pabelick,[‡,§] Resham Bhattacharya,[†] J. David Robertson,[#] Vincent M. Rotello,[⊥] Y. S. Prakash,[*,‡,§] and Priyabrata Mukherjee[*,†,§,∥]

[†]Department of Biochemistry and Molecular Biology, [‡]Department of Anesthesiology, [§]Department of Physiology and Biomedical Engineering, and [∥]Mayo Clinic Cancer Center, Mayo Clinic College of Medicine, Rochester, Minnesota 55905, [⊥]Department of Chemistry, University of Massachusetts, Amherst, Massachusetts 01003, and [#]Department of Chemistry and University of Missouri Research Reactor, University of Missouri, Columbia, Missouri 65211

ABSTRACT Herein, we demonstrate that the surface charge of gold nanoparticles (AuNPs) plays a critical role in modulating membrane potential of different malignant and nonmalignant cell types and subsequent downstream intracellular events. The findings presented here describe a novel mechanism for cell-nanoparticle interactions and AuNP uptake: modulation of membrane potential and its effect on intracellular events. These studies will help understand the biology of cell-nanoparticle interactions and facilitate the engineering of nanoparticles for specific intracellular targets.

KEYWORDS Gold nanoparticles, surface properties, cancer, membrane potential, calcium, apoptosis

In recent years, significant effort has been devoted to develop nanotechnology for the delivery of small molecular weight drugs, as well as macromolecules such as proteins, peptides, or genes into cells and tissue.[1−7] Targeted nanoparticle-mediated drug delivery may be used to direct the particles to specific tissues (minimizing toxicity), improve oral bioavailability, sustain drug/gene effect in the target tissue, solubilize drugs for intravascular delivery, and/or improve the stability of therapeutic agents against enzymatic degradation.[8] Despite the fantastic potential for nanoparticle use in medicine, fundamental studies to understand the molecular interactions of nanoparticles with their target cells (normal as well as malignant) remain largely unexplored. One such mechanism of action may be ionic interactions; the negative membrane potential of most cells likely interacts differently with nanoparticles of a positive versus negative charge density. These interactions could, in turn, determine intracellular uptake and localization of the nanoparticles and their biological functions. Understanding such interactions between cells and nanoparticles with different surface properties is important not only for engineering of nanoparticles that exhibit selective intracellular uptake (to subsequently modulate cellular processes of interest) but also for determining the relative cytotoxicity of nanoparticles.

All living cells have an inherent membrane potential that is determined by ionic permeability and modulated by processes including electrical or agonist stimulation, ion channels, and changes in intracellular versus extracellular ionic concentrations. Furthermore, the membrane potential itself can modulate a number of intracellular pathways, including intracellular Ca^{2+} concentration ($[Ca^{2+}]_i$), the cell cycle, and cellular proliferation versus apoptosis; each important not only for normal cell structure and function but also in the progression of diseases, especially cancer.[9,10] Additionally, changes in $[Ca^{2+}]_i$ induced by altered membrane potential or by other mechanisms serves to regulate cell growth. Accordingly, if nanoparticles are to realize their potential in biomedical applications it is important to determine the nature of their interactions with cells (particularly the plasma membrane), and their concomitant modulation of subsequent signaling pathways (especially $[Ca^{2+}]_i$ regulation). We address here these important issues in nanoparticle biology by testing the hypothesis that membrane potential is a key player in determining intracellular uptake of nanoparticles. Using both malignant cells (ovarian cancer CP70 and A2780 cells) and nonmalignant, excitable cells (human bronchial epithelial cells (BECs) and human airway smooth muscle (ASM) cells), we investigated whether cellular membrane potential plays a role in uptake of gold nanoparticles (AuNPs) of different charges (positive, $^{+}$AuNP; negative, $^{-}$AuNP; neutral, ^{0}AuNP; and zwitterionic, $^{\pm}$AuNP; Figure 1A), and likewise quantified the subsequent effects on $[Ca^{2+}]_i$ and cellular proliferation versus apoptosis.

To assess the role of surface charge of nanoparticles on membrane potential, we synthesized AuNPs (∼2 nm core size) using the Brust-Schiffrin two-phase synthesis method.[11,12] Surface functionalization was achieved via the Murray place-exchange method.[13] These particles were applied to CP70,[14]

* To whom correspondence should be addressed. (P.M.) Department of Biochemistry and Molecular Biology, Gugg 1321B, College of Medicine, Mayo Clinic, 200 First St SW, Rochester, MN 55905. E-mail: Mukherjee.priyabrata@mayo.edu. (Y.S.P.) Department of Anesthesiology, 4-184 W Jos SMH, College of Medicine, Mayo Clinic, 200 First St SW, Rochester, MN 55905. E-mail: prakash.ys@mayo.edu.

Received for review: 03/31/2010
Published on Web: 06/10/2010

DOI: 10.1021/nl101140t | *Nano Lett.* **2010,** *10,* 2543–2548

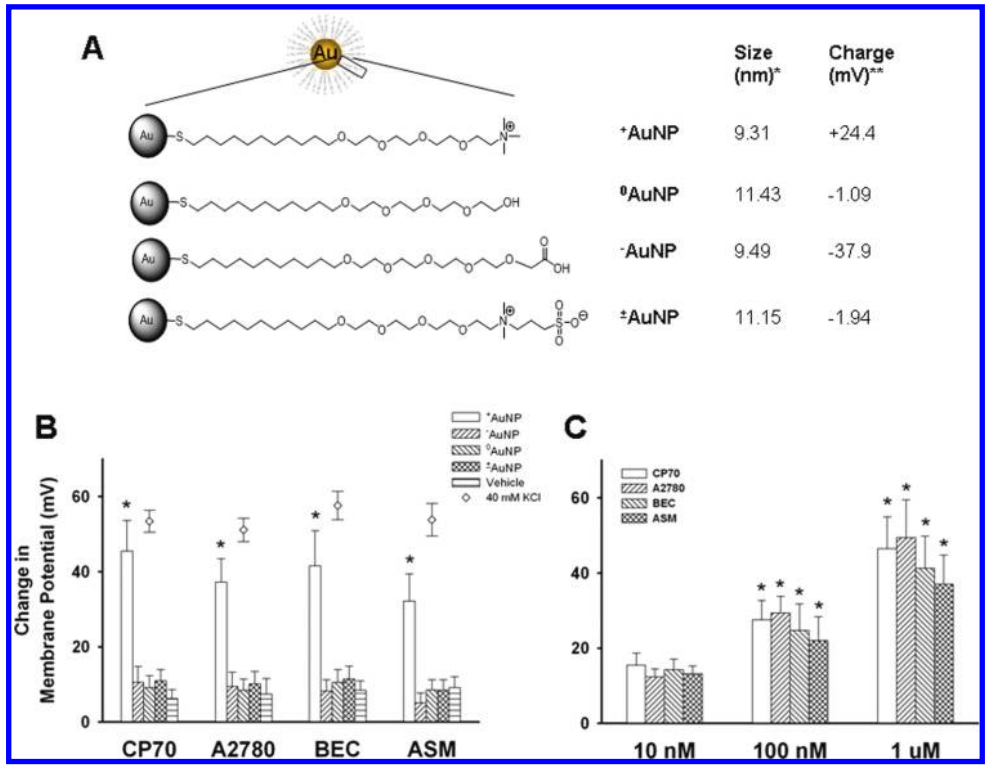

FIGURE 1. Summary of AuNPs effects on cellular membrane potential. AuNPs of different surface charges were generated by chemical modification of the terminal portion of the ligand bonded to the nanoparticle core. Four types of AuNPs were examined (A): neutral (^{0}AuNP), positive ($^+$AuNP), negative ($^-$AuNP), and zwitterionic ($^\pm$AuNP). The diameter (*) and surface charge (**) were measured by dynamic light scattering and ζ-potential, respectively. Using the cell-permeant fluorescent membrane potential indicator RH414 and real-time fluorescence microscopy, membrane potential changes following exposure to AuNPs of different surface charges were measured for two ovarian cancer cell lines (CP70, A2780), human bronchial epithelial cells (BEC), and human airway smooth muscle (ASM) cells (also see Supporting Information Figure S1). $^+$AuNPs (1.2 μM) produced rapid and significant membrane depolarization (panel B; bars; comparable to that induced by 40 mM KCl, diamonds). The extent of membrane potential change was dependent on $^+$AuNPs concentration (C) with minimal changes at 10 nM. In comparison to $^+$AuNPs, those with other charges had negligible effects on membrane potential in any cell type (B). Values are means ±SE. * indicates significant AuNP effect ($p < 0.05$).

A2780, BEC,[15] and ASM[16] cells loaded with the fluorescent, fast-response membrane potential-sensitive dye RH414. The baseline plasma membrane potential ranged between −75 and −55 mV depending on cell type. With images taken at 1−2 frames/s, fluorescence levels remained stable for at least 5 min in vehicle controls.[16] Among the four species of AuNPs, only $^+$AuNPs induced membrane depolarization across different cell types (Figure 1B). In comparison, membrane depolarization induced by $^-$AuNP, ^{0}AuNP or $^\pm$AuNP was negligible (Figure 1B, also see Supporting Information Figure S1). The extent of membrane depolarization was found to be dependent on $^+$AuNP concentration (Figure 1C; $p < 0.05$ compared to vehicle control) with minimal depolarization at 10 nM, and substantial depolarization at 1.2 μM $^+$AuNP in less than 10 s with maximum depolarization reached in ∼5 min across cell types (Supporting Information Figure S1). Among cell types, the extent of depolarization was greatest in ovarian cancer cells (CP70, A2780) and comparable to that achieved with 40 mM KCl (which produces a depolarization to ∼−25 mV) (Figure 1B, and Supporting Information Figure S1). We verified lack of fluorescence quenching by examining the effect of AuNPs on RH414 fluorescence in an in vitro acellular preparation (not shown).

Next, we wanted to investigate the factors that determined intracellular uptake of AuNPs, focusing on membrane potential. In CP70, A2780, BEC, and ASM cells, uptake of $^+$AuNPs (as determined by INAA[17]) was significantly higher than AuNPs of other charges (Figure 2A; $p < 0.05$). However, prior depolarization of the plasma membrane using 40 or 80 mM KCl (which changed membrane potential to ∼−25 and ∼−8 mV, respectively) resulted in significant reduction in the extent of $^+$AuNP uptake in all cell types (Figure 2B; $p < 0.05$). Furthermore, in cells pre-exposed to KCl, the extent of membrane depolarization induced by 1.2 μM $^+$AuNPs was significantly smaller, confirming the inability of these particles to depolarize the membrane under these conditions (Figure 2C; $p < 0.05$). In summary, these data clearly demonstrate a key role for membrane potential in intracellular uptake of AuNPs. Furthermore, by altering membrane potential, AuNPs may modulate their own uptake.

In most cells, membrane depolarization leads to increases in $[Ca^{2+}]_i$ that can result in further modulation of cellular events (such as proliferation vs apoptosis).[9,18] To test whether such membrane depolarization by $^+$AuNPs and their intracellular uptake had any effect on intracellular signaling events, we first determined changes in $[Ca^{2+}]_i$. In CP70,

DOI: 10.1021/nl101140t | *Nano Lett.* **2010,** *10,* 2543--2548

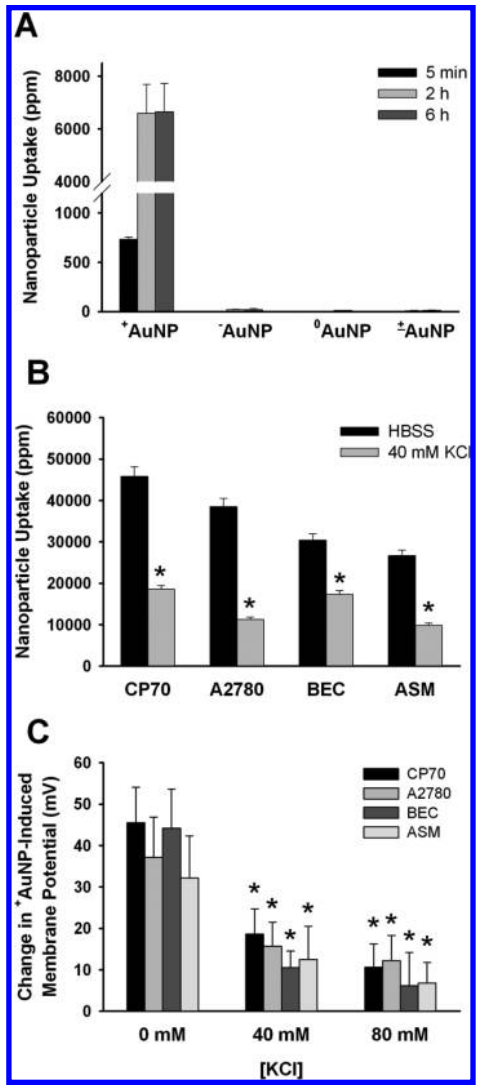

FIGURE 2. AuNP uptake and membrane potential. (A) In CP70 cells, only $^{+}$AuNPs (0.4 μM) showed significant uptake, with substantial intracellular levels present at 5 min, followed by a higher level beyond 2 h. (B) Prior exposure to KCl (inducing membrane depolarization) significantly ($p < 0.05$) reduced the extent of uptake of $^{+}$AuNPs (1.2 μM for 30 min treatment) in four different types of cells. (C) In all the cells investigated, prior exposure to KCl significantly blunted the extent of membrane depolarization subsequently induced by $^{+}$AuNPs. Values are means ±SE. * indicates significant AuNP effect ($p < 0.05$).

A2780, BEC, and ASM cells loaded with the ratiometric fluorescent Ca^{2+}-sensitive dye fura-2/AM, baseline $[Ca^{2+}]_i$ ranged between 75 and 120 nM (depending on cell type). In conformity with changes in membrane potential, addition of 1.2 μM $^{+}$AuNP to CP70 and A2780 cells resulted in immediate and sustained increases in $[Ca^{2+}]_i$ while in BEC and ASM cells, the increase in $[Ca^{2+}]_i$ was slightly delayed. In all cell types, $[Ca^{2+}]_i$ levels increased rapidly to a plateau level (Supporting Information Figure S2), with maximum $[Ca^{2+}]_i$ reached in ~5 min (Figure 3A). Some cells displayed an initial higher $[Ca^{2+}]$, followed by a decay to a lower level above baseline (Supporting Information Figure S2). Addition of AuNPs of other surface charges produced negligible changes in $[Ca^{2+}]_i$ levels (Figure 3A,B and Supporting Information Figure S2). In control experiments, each of these cell types were exposed to 40 mM KCl, which produced $[Ca^{2+}]_i$ elevations across cell types albeit with different time delays and profiles (Supporting Information Figure S2). The extent of change in $[Ca^{2+}]_i$ was concentration-dependent with significant changes observed even at 10 nM $^{+}$AuNPs (Figure 3C; $p < 0.05$). As with RH414, lack of fura-2 quenching by AuNPs was verified using the cell-impermeant pentapotassium form of fura-2 (not shown).

To determine the temporal relationship between membrane depolarization and elevated $[Ca^{2+}]_i$, we simultaneously visualized both parameters by loading cells with RH414 and the nonratiometric Ca^{2+} indicator fluo-3/AM. Immediately following exposure to $^{+}$AuNPs, distinct membrane depolarization occurred, prior to any changes in $[Ca^{2+}]_i$ (not shown). As membrane potential reached ~−30 mV, increases in $[Ca^{2+}]_i$ were observed. Clearly, the membrane potential had reached a maximum state of depolarization prior to maximum changes in $[Ca^{2+}]_i$. The temporal relationship between depolarization and $[Ca^{2+}]_i$ was further verified using 40 or 80 mM KCl, which induced RH414 changes prior to increasing $[Ca^{2+}]_i$ detected using fluo-3. In this regard, the change in +AuNP-induced changes in membrane potential and $[Ca^{2+}]_i$ were comparable to that by 40 mM KCl. Taken together, these data links membrane depolarization induced by $^{+}$AuNPs to increased $[Ca^{2+}]_i$.

A number of mechanisms regulate $[Ca^{2+}]_i$ with the relative contribution of plasma membrane versus intracellular mechanisms differing between cell types.[19,20] Indeed, it is now recognized that a number of disease states involve dysregulation of this universal intracellular messenger, modulating cellular proliferation versus apoptosis (as in cancers and other proliferative diseases), cellular contraction (as in asthma and other reactive airway diseases), and fibrosis.[9,10,16,20,21] Accordingly, we determined the mechanisms by which AuNPs modulate $[Ca^{2+}]_i$. This was performed in CP70 cells by first inhibiting specific Ca^{2+} regulatory mechanisms and then exposing cells to 1.2 μM $^{+}$AuNPs (Figure 3D). Inhibition of plasma membrane voltage-gated Ca^{2+} influx via L-type Ca^{2+} channels (using nifedipine) resulted in a reduction in $^{+}$AuNP effects on $[Ca^{2+}]_i$ levels (Figure 3D), indicating a significant contribution via this mechanism, especially given that $^{+}$AuNP induces membrane depolarization. $^{+}$AuNP effects on $[Ca^{2+}]_i$ were even more blunted in the absence of extracellular Ca^{2+} (0 Ca HBSS) suggesting that Ca^{2+} influx via mechanisms other than L-type channels contributes to the observed change in $[Ca^{2+}]_i$ with $^{+}$AuNPs. The remainder of the $[Ca^{2+}]_i$ response may be derived either from endoplasmic reticulum (ER) or mitochondria (since some of the response persists in the absence of extracellular Ca^{2+}). To distinguish between these effects, inhibitors of the two well-known ER Ca^{2+} release channels (inositol trisphosphate (IP_3) receptor channels inhibited by Xestospongin C, and ryanodine receptor (RyR) channels inhibited by high ryanodine

DOI: 10.1021/nl101140t | *Nano Lett.* **2010,** *10,* 2543--2548

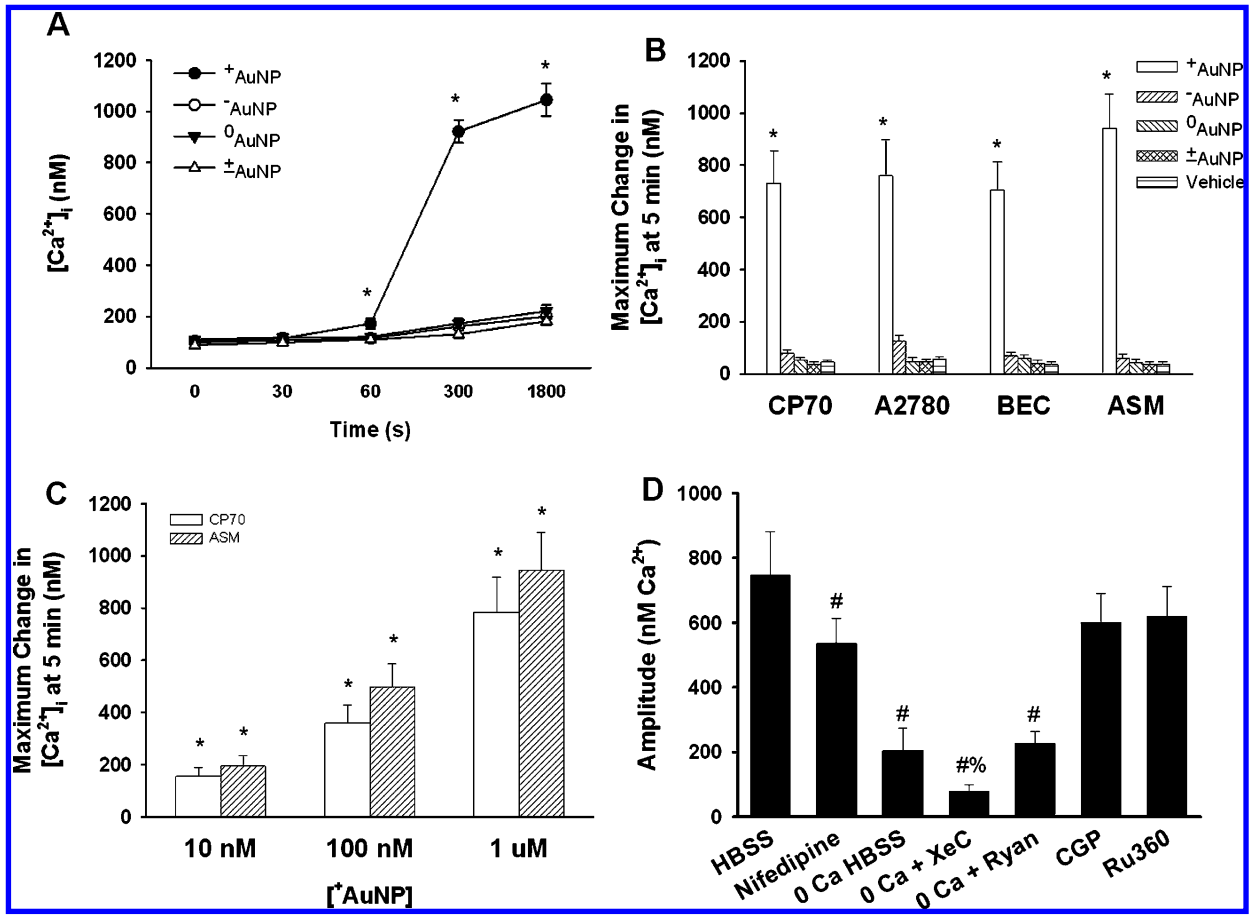

FIGURE 3. Summary of $^{+}$AuNPs effects on intracellular Ca^{2+} ($[Ca^{2+}]_i$) levels. (A,B) In ovarian cancer cells (CP70, A2780) and airway cells (BEC, ASM) loaded with the ratiometric fluorescent Ca^{2+} indicator fura-2, $^{+}$AuNPs (1.2 μM) produced substantial increases in $[Ca^{2+}]_i$ levels that reached a maximum value in ~5 min and in some cell types decayed to a lower level above baseline (see Supporting Information Figure S2). In comparison, AuNPs with other charges had negligible effects on $[Ca^{2+}]_i$ levels. The effect on $[Ca^{2+}]_i$ levels was dependent on the concentration of $^{+}$AuNPs (C) with even 10 nM AuNPs producing a substantial increase in $[Ca^{2+}]_i$ (compared to small effects on membrane potential). In ovarian cancer CP70 cells, the role of specific $[Ca^{2+}]_i$ regulatory mechanisms were examined by first inhibiting specific Ca^{2+} regulatory mechanisms, and then exposing cells to $^{+}$AuNPs (1.2 μM) (D). Inhibition of plasma membrane Ca^{2+} influx via L-type Ca^{2+} channels resulted in significant reduction in positively charged AuNP effects on $[Ca^{2+}]_i$ levels. AuNP effects were even more reduced in the absence of extracellular Ca^{2+} (0 Ca HBSS) suggesting that Ca^{2+} influx (partly via L-type channels) contributes to the observed change in $[Ca^{2+}]_i$ levels with AuNPs. The remainder of the $[Ca^{2+}]_i$ response appears to be derived from endoplasmic reticulum Ca^{2+} release (since the response persists in the absence of extracellular Ca^{2+}) especially via IP3 receptor channels (evidenced by lack of AuNP effects when the channels are inhibited by Xestospongin C). Lack of effect of mitochondrial Ca^{2+} pathways (CGP 37,157 for mitochondrial $Na+/Ca^{2+}$ exchange and Ru360 for mitochondrial Ca^{2+} uniporter) suggests that AuNPs may not be affecting mitochondria. Values are means ±SE. * indicates significant AuNP effect, # indicates significant effect of 0 Ca HBSS, and % indicates significant effect of inhibitor ($p < 0.05$).

concentrations),[19] and of mitochondrial Ca^{2+} pathways (Ca^{2+} uniporter inhibited by Ru360, and mitochondrial Na^{+}/Ca^{2+} exchange inhibited by CGP 37,157)[22−24] were used. In the presence of Xestospongin C (but in the absence of extracellular Ca^{2+}), $^{+}$AuNP-induced increase in $[Ca^{2+}]_i$ was small, confirming a role for Ca^{2+} release from ER stores via these channels. In comparison, blocking RyR channels had no effect. The lack of effect of mitochondrial Ca^{2+} pathway inhibitors (Ru360 and CGP 37,157) suggests that AuNPs may not be affecting mitochondrial Ca^{2+} regulation. Overall, these data suggest that $^{+}$AuNPs elevate $[Ca^{2+}]_i$ by stimulating plasma membrane Ca^{2+} influx and ER Ca^{2+} release.

Finally we wanted to investigate whether $^{+}$AuNP modulation of membrane potential and $^{+}$AuNP uptake affects cellular proliferation or viability. $^{+}$AuNPs completely inhibited proliferation (determined by ^{3}H-thymidine incorporation[4]) of BECs, whereas proliferation of CP70 and A2780 cells remained largely unaffected (Figure 4A; $p > 0.05$). Furthermore, apoptosis (determined using annexin-propidium iodide assay) was only slightly increased in CP70 cells following $^{+}$AuNP exposure (Figure 4B). In contrast, BEC cells displayed substantial apoptosis (Figure 4B; $p < 0.05$). Indeed, cellular viability (determined by an MTS assay) of normal BEC and ASM cells was substantially reduced by $^{+}$AuNP exposure (Figure 4C; $p < 0.05$). To determine whether these changes in cellular proliferation and apoptosis were a result of $^{+}$AuNP-induced membrane depolarization and $[Ca^{2+}]_i$ elevation, we performed control studies where 40 or 80 mM KCl was used to induced membrane potential and $[Ca^{2+}]_i$ changes. Cells were exposed to KCl only for 5 or 30 min (to transiently induce

DOI: 10.1021/nl101140t | Nano Lett. 2010, 10, 2543--2548

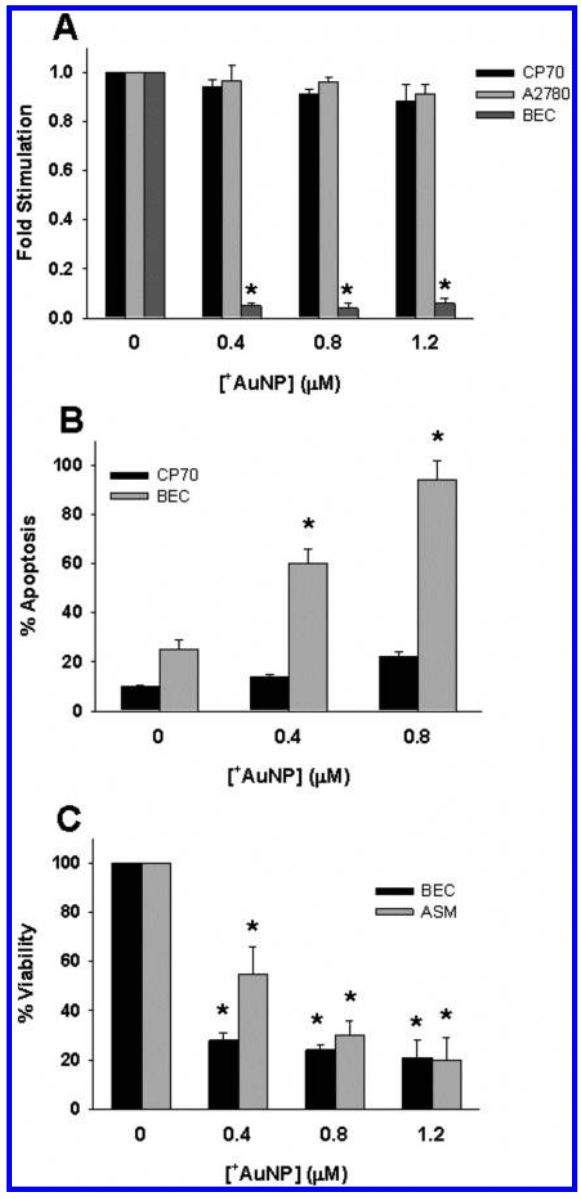

FIGURE 4. Effect of AuNPs on cellular proliferation versus apoptosis. (A) Even brief (30 min) exposure of cells to $^{+}$AuNPs substantially blunted the proliferation of human BECs, but it did not affect the proliferation of ovarian cancer CP70 or A2780 cells. (B). Apoptosis of BEC by $^{+}$AuNPs was concentration-dependent and substantial. In contrast, some degree of apoptosis (<10%) of CP70 cells occurred only at a higher $^{+}$AuNP concentration. (C) The viability of both BECs and ASM cells was substantially reduced by $^{+}$AuNPs, with a concentration-dependence for ASM. * indicates significant effect ($p < 0.001$).

$[Ca^{2+}]_i$ changes) to mimic $^{+}$AuNP exposure. Compared to $^{+}$AuNPs, KCl induced substantially lesser apoptosis and affected proliferation of BECs to a lesser extent (Supporting Information Figure S3, compare to Figure 4). Furthermore, unlike $^{+}$AuNPs, KCl had negligible effects on apoptosis of ASM cells. In all of these experiments, it must be noted that the duration of AuNP (or KCl) exposure was brief (minutes), while apoptosis or proliferation was evaluated after ~24 h (overnight). Accordingly, these changes are unlikely to reflect short-term cell death resulting from cytotoxicity of AuNPs.

These novel data highlight several characteristics of $^{+}$AuNPs: (1) uptake of $^{+}$AuNPs results in substantial inhibition of proliferation and decreased viability of normal cells, but not of cancer cells, even though comparable membrane depolarization and increased $[Ca^{2+}]_i$ occurs across cell types. These differential effects of $^{+}$AuNPs on normal versus malignant cells, and their potential relevance to nanoparticle design and applications are interesting and require further investigation; (2) the fact that within a cell type (e.g., BECs), $^{+}$AuNP effects on proliferation, apoptosis, or viability are greater than that of KCl only (in spite of comparable depolarization or $[Ca^{2+}]_i$ elevation) indicates that $^{+}$AuNP effects on cells are mediated not only via altered membrane potential and $[Ca^{2+}]_i$, but additional effects on signaling pathways. Accordingly, an important aspect of understanding AuNP action may be identifying different signaling mechanisms that may be targeted by AuNPs, with normal versus cancer cells being differently sensitive to alterations in these mechanisms (especially relating to apoptosis and proliferation).

In conclusion, we have demonstrated that cellular membrane potential plays a prominent role in intracellular uptake of AuNPs. Perturbation of the membrane potential is dependent on surface charge of the nanoparticles; positively charged nanoparticles depolarize the membrane to the greatest extent with nanoparticles of other charges having negligible effect. Such membrane potential perturbations result in increased $[Ca^{2+}]_i$, which in turn inhibits the proliferation of normal cells whereas malignant cells remain unaffected. The mechanisms by which positively charged nanoparticles interact with the plasma membrane need to be further investigated. Such interactions may involve AuNPs binding to the plasma membrane. Indeed, this was found using transmission electron microscopy[25] (TEM) where nanoparticles were clearly seen to be bound to the cell membrane (Figures 5A, left panels are the low magnification images, right panels being the higher magnification images of the corresponding left panels). Once bound to the plasma membrane, an obvious question is whether AuNPs disrupt the membrane, potentially resulting in depolarization and Ca^{2+} influx. However, TEM studies did not demonstrate any membrane disruption (Figure 5A). One plausible mechanism for AuNP action is the flipping of membrane areas by these particles. Uptake may also involve lipid rafts, pinocytosis and other plasma membrane mechanisms. Indeed, previous studies have found that modulation of nanoparticle surface properties can influence the mechanism of intracellular uptake (i.e., endosomal, passive diffusion).[26−28] However, the extremely fast membrane depolarization and rapid uptake of AuNPs that was observed in our study need to be reconciled with the relatively slow rate of such uptake processes. Regardless, the findings of the present study will help to better define the biology of cell-nanoparticle interactions and help engineer nanoparticles to modulate cellular functions of interest. For example, varying surface charge density or combining positive and negative charges on the same nanoparticle may allow for graduated cellular uptake, targeting toward specific intracellular organelles, as well as control of the extent of change in $[Ca^{2+}]_i$

DOI: 10.1021/nl101140t | *Nano Lett.* **2010,** *10,* 2543--2548

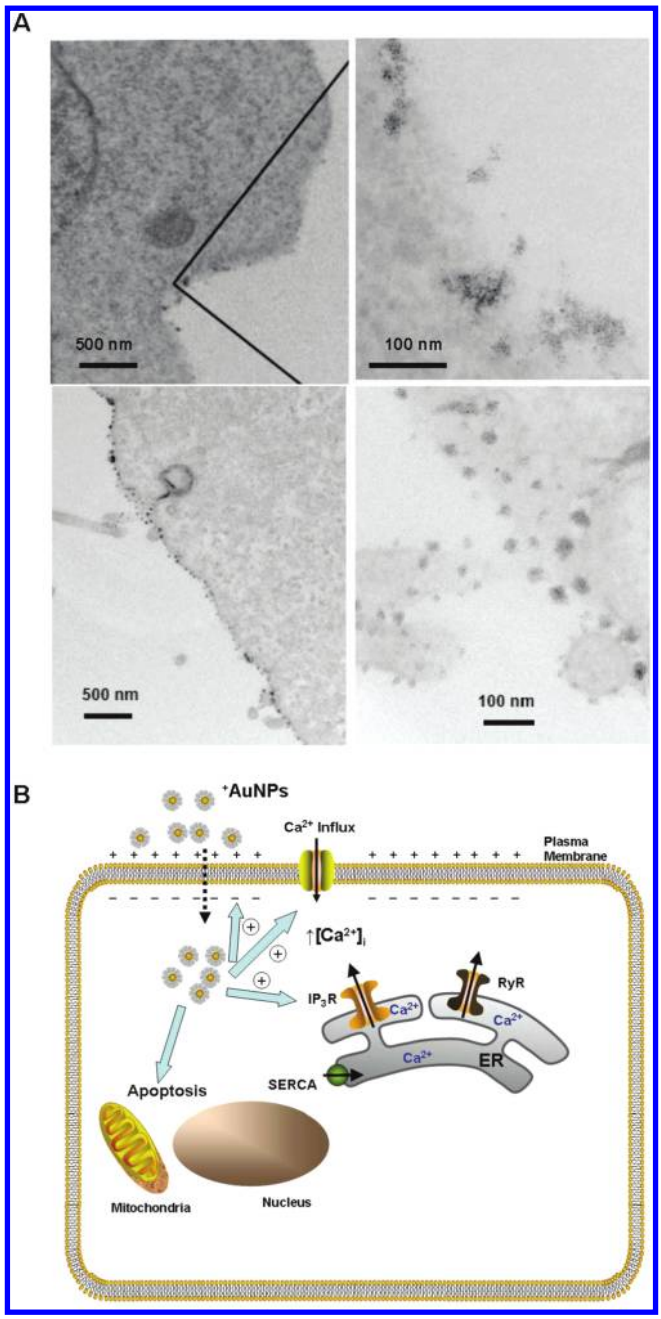

FIGURE 5. (A) Transmission electron microscopy of $^{+}$AuNP (concentration = 0.4 μM) interactions with plasma membrane. Top panels demonstrate localization of $^{+}$AuNPs within the plasma membrane (CP70 cells). Bottom panels demonstrate lack of plasma membrane disruption following $^{+}$AuNP uptake (BEC cells). (B) Schematic of AuNP effects on cellular function. On the basis of our findings using $^{+}$AuNPs and different types of cells, we propose that AuNPs are taken up intracellularly, based on membrane potential. Upon uptake, $^{+}$AuNPs produce membrane depolarization, and increase $[Ca^{2+}]_i$ by enhancing Ca^{2+} influx and inducing release of intracellular Ca^{2+} stores (e.g., via IP_3 receptor channels of the endoplasmic reticulum; ER). These changes can result in increased apoptosis and decreased cellular proliferation, depending on cell type. Further modulation of apoptosis and proliferation may involve direct nanoparticle effects on intracellular signaling mechanisms.

and other effects, thus balanced unintended cytotoxicity versus targeting mechanisms of interest.

Acknowledgment. Supported by NIH CA135011, CA136494, and UTMD-1 Grants (P.M.) and by NIH Grants HL090595 (C.M.P.), GM077173 (V.M.R.), and HL088029 (Y.S.P.).

Supporting Information Available. Materials and methods; additional data. This material is available free of charge via the Internet at http://pubs.acs.org.

REFERENCES AND NOTES

(1) Ferrari, M. *Nat. Rev. Cancer* **2005**, *5* (3), 161–71.
(2) Burda, C.; Chen, X.; Narayanan, R.; El-Sayed, M. A. *Chem. Rev.* **2005**, *105* (4), 1025–102.
(3) Daniel, M. C.; Astruc, D. *Chem. Rev.* **2004**, *104* (1), 293–346.
(4) Patra, C. R.; Bhattacharya, R.; Wang, E.; Katarya, A.; Lau, J. S.; Dutta, S.; Muders, M.; Wang, S.; Buhrow, S. A.; Safgren, S. L.; Yaszemski, M. J.; Reid, J. M.; Ames, M. M.; Mukherjee, P.; Mukhopadhyay, D. *Cancer Res.* **2008**, *68* (6), 1970–8.
(5) Mirkin, C. A.; Taton, T. A. *Nature* **2000**, *405* (6787), 626–7.
(6) Alivisatos, P. *Nat. Biotechnol.* **2004**, *22* (1), 47–52.
(7) Whitesides, G. M. *Nat. Biotechnol.* **2003**, *21* (10), 1161–5.
(8) Xu, P.; Van†Kirk, E. A.; Zhan, Y.; Murdoch, W. J.; Radosz, M.; Shen, Y. *Angew. Chem., Int. Ed.* **2007**, *46* (26), 4999–5002.
(9) Monteith, G. R.; McAndrew, D.; Faddy, H. M.; Roberts-Thomson, S. J. *Nat. Rev. Cancer* **2007**, *7* (7), 519–530.
(10) Prevarskaya, N.; Skryma, R.; Shuba, Y. Trends Mol. Med., in press.
(11) Brust, M.; Walker, M.; Bethell, D.; Schiffrin, D. J.; Whyman, R. J. *J. Chem. Soc., Chem. Commun.* **1994**, 801–802.
(12) Kanaras, A. G.; Kamounah, F. S.; Schaumburg, K.; Kiely, C. J.; Brust, M. *Chem. Commun.* **2002**, 2294–2295.
(13) Templeton, A. C.; Wuelfing, W. P.; Murray, R. W. *Acc. Chem. Res.* **2000**, *33*, 27.
(14) Behrens, B. C.; Hamilton, T. C.; Masuda, H.; Grotzinger, K. R.; Whang-Peng, J.; Louie, K. G.; Knutsen, T.; McKoy, W. M.; Young, R. C.; Ozols, R. F. *Cancer Res.* **1987**, *47* (2), 414–418.
(15) Fulcher, M. L.; Gabriel, S.; Burns, K. A.; Yankaskas, J. R.; Randell, S. H. *Methods Mol. Med.* **2005**, *107*, 183–206.
(16) Prakash, Y. S.; Thompson, M. A.; Pabelick, C. M. *Am. J. Respir. Cell Mol. Biol.* **2009**, *41* (5), 603–11.
(17) Kattumuri, V.; Katti, K.; Bhaskaran, S.; Boote, E. J.; Casteel, S. W.; Fent, G. M.; Robertson, D. J.; Chandrasekhar, M.; Kannan, R.; Katti, K. V. *Small* **2007**, *3* (2), 333–341.
(18) Chakrabarti, R. *J. Cell Biochem.* **2006**, *99* (6), 1503–16.
(19) Pabelick, C. M.; Sieck, G. C.; Prakash, Y. S. *J. Appl. Physiol.* **2001**, *91* (1), 488–96.
(20) Perez-Zoghbi, J. F.; Karner, C.; Ito, S.; Shepherd, M.; Alrashdan, Y.; Sanderson, M. J. *Pulm. Pharmacol. Ther.* **2009**, *22* (5), 388–97.
(21) Sathish, V.; Thompson, M. A.; Bailey, J. P.; Pabelick, C. M.; Prakash, Y. S.; Sieck, G. C. *Am. J. Physiol. Lung Cell Mol. Physiol.* **2009**, *297* (1), L26–34.
(22) Balemba, O. B.; Bartoo, A. C.; Nelson, M. T.; Mawe, G. M. *Am. J. Physiol. Gastrointest. Liver Physiol.* **2008**, *294* (2), G467–476.
(23) Michels, G. M. K.; Ismail, F.; Endres-Becker, J.; Rottlaender, D.; Herzig, S.; Ruhparwar, A.; Wahlers, T.; Hoppe, U. C. *Circulation* **2009**, *119* (18), 2435–2443.
(24) Liu, T.; Brown, D. A.; O'Rourke, B. *Biophys. J.* **2009**, *96* (3), 243a–243a.
(25) Bhattacharya, R.; Patra, C. R.; Earl, A.; Wang, S.; Katarya, A.; Lu, L.; Kizhakkedathu, J. N.; Yaszemski, M. J.; Greipp, P. R.; Mukhopadhyay, D.; Mukherjee, P. *Nanomedicine* **2007**, *3*, 224–238.
(26) Verma, A.; Uzun, O.; Hu, Y.; Hu, Y.; Han, H.-S.; Watson, N.; Chen, S.; Irvine, D. J.; Stellacci, F. *Nat. Mater.* **2008**, *7* (7), 588–595.
(27) Leroueil, P. R.; Hong, S.; Mecke, A.; Baker, J. R.; Orr, B. G.; Banaszak Holl, M. M. *Acc. Chem. Res.* **2007**, *40* (5), 335–342.
(28) Verma, A.; Stellacci, F. *Small* **2010**, *6* (1), 12–21.

DOI: 10.1021/nl101140t | *Nano Lett.* **2010,** *10,* 2543–2548